A fast and stable explicit operator splitting method for phase-field models

Yuanzhen Cheng[1], Alexander Kurganov[1], Zhuolin Qu[1] and Tao Tang[2]

[1] Mathematics Department, Tulane University [2] Department of Mathematics, Hong Kong Baptist University

Goal

Develop fast and reliable numerical algorithms for phase-field models:

- molecular beam epitaxy (MBE) equation with slop selection

$$u_t = -\delta\Delta^2 u - \nabla\cdot[(1-|\nabla u|^2)\nabla u], \quad \boldsymbol{x}\in\Omega\subset\mathbb{R}^2$$

- Cahn-Hilliard (CH) equation

$$u_t = -\delta\Delta^2 u + \Delta(u^3-u), \quad \boldsymbol{x}\in\Omega\subset\mathbb{R}^2$$

subject to periodic boundary conditions.

What are phase-field models?

Phase-field models are mathematical models to solve interfacial problems:

Thin film epitaxy the deposition of a crystalline overlayer on a crystalline substrate → MBE equation (Figure 1 left)

Phase separation two components of a binary fluid spontaneously separate and form domains pure in each component → CH equation (Figure 1 right [5])

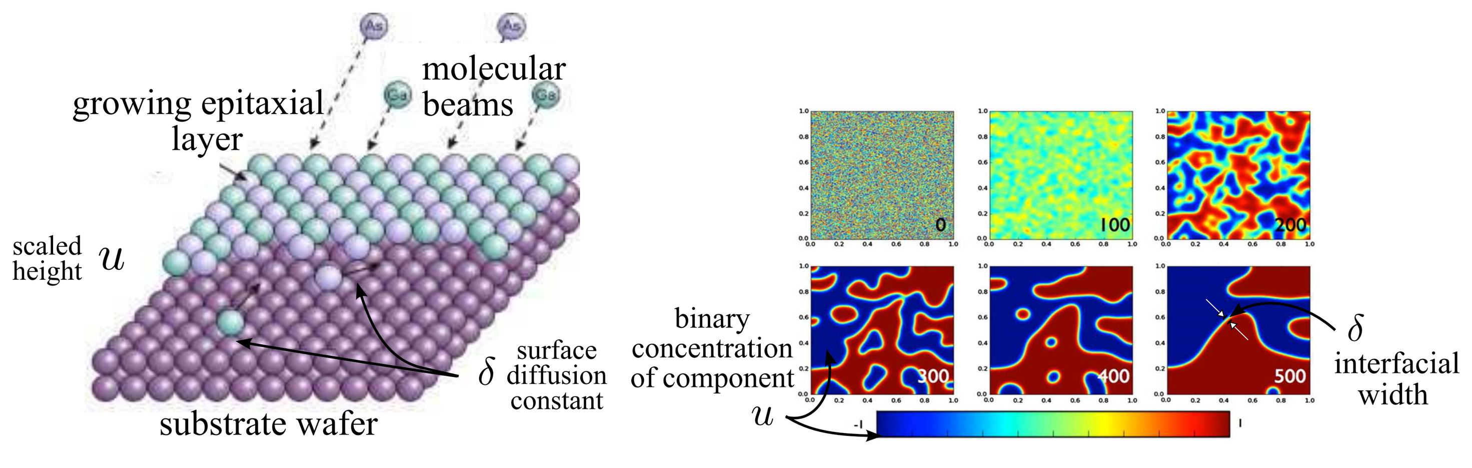

Figure 1: MBE (left): thin film epitaxy; CH equation (right): phase separation

Numerical challenges

To numerically solve the models, we have following potential numerical difficulties:

severe timestep restriction (accuracy)

To accurately resolve dynamics, the perturbed biharmonic operator $\delta\Delta^2(\cdot)$, which is involved in the governing equations, may lead to severe restriction on numerical timestep selection.

long-time simulations (efficiency)

Numerical simulations of phase-field models require long time computations to attain the steady states (equilibria) of the corresponding phase-field models.

nonlinear energy stability

Strong nonlinearities within energy (defined below) are intrinsic in phase-field models. Violating the energy stability may lead to nonphysical oscillations.

- $$E_{\rm MBE}(u) = \int_\Omega\left[\frac{\delta}{2}|\Delta u|^2 + \frac{1}{4}(|\nabla u|^2-1)^2\right]d\boldsymbol{x}.$$
- $$E_{\rm CH}(u) = \int_\Omega\left[\frac{\delta}{2}|\nabla u|^2 + \frac{1}{4}(u^2-1)^2\right]d\boldsymbol{x}.$$

⇓

balance among solution accuracy, efficiency and nonlinear stability

Operator splitting methods

- MBE equation:

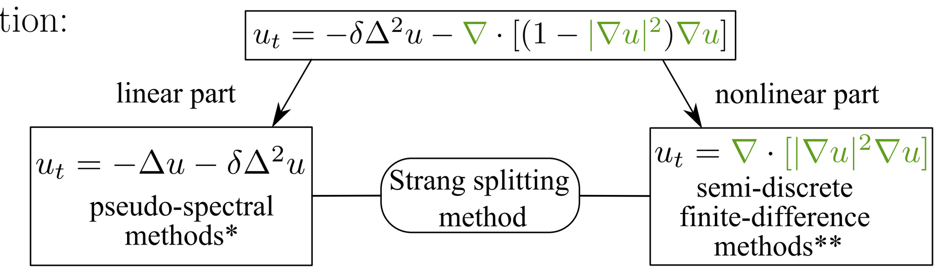

Figure 2: Numerical algorithm for MBE equation

∗ pseudo-spectral method with fast-fourier transform (FFT):

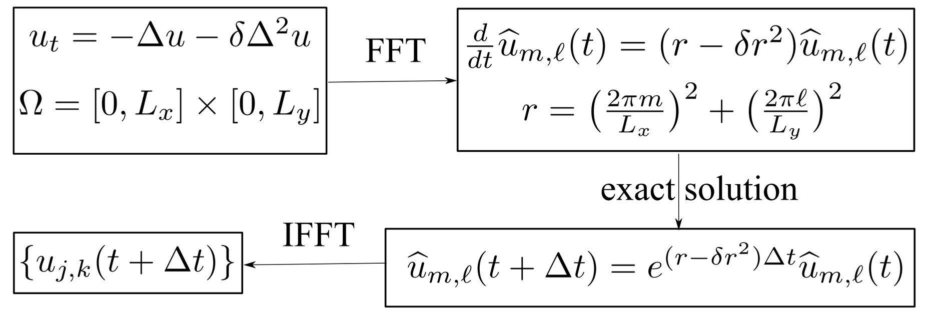

∗∗ $2\,m^{th}$-order finite-difference approximations of the nonlinear part:

$$\frac{du_{j,k}}{dt} = \sum_{p=-m}^{m}\alpha_p H^x_{j+p,k} + \sum_{p=-m}^{m}\beta_p H^y_{j,k+p}$$

where $\{\alpha_p\}$ and $\{\beta_p\}$ are coefficients of the $2\,m^{th}$-order centered finite-difference approximations

$$(u_x)_{j,k} := \sum_{p=-m}^{m}\alpha_p u_{j+p,k} \quad (u_y)_{j,k} := \sum_{p=-m}^{m}\beta_p u_{j,k+p}$$

$$H^x_{j,k} := [(u_x)^2_{j,k} + (u_y)^2_{j,k}](u_x)_{j,k} \quad H^y_{j,k} := [(u_y)^2_{j,k} + (u_x)^2_{j,k}](u_y)_{j,k}$$

- CH equation:

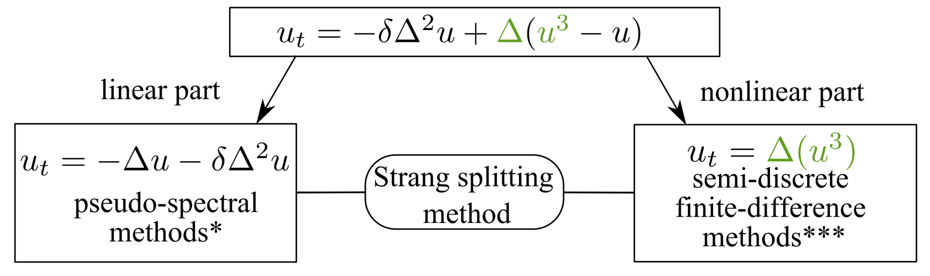

Figure 3: Numerical algorithm for CH equation

∗∗∗ $2\,m^{th}$-order finite-difference approximations of the nonlinear part:

$$H^x_{j,k} = \sum_{p=-m}^{m}\alpha_p u^3_{j+p,k} \quad \text{and} \quad H^y_{j,k} = \sum_{p=-m}^{m}\beta_p u^3_{j,k+p}$$

Explicit ODE solver for nonlinear parts

Efficient explicit and stable ODE solver *DUMKA3* [4]:

large stability domain

It belongs to a class of Runge-Kutta-Chebyshev method and allows one to use much larger timesteps compared with the standard Runge-Kutta methods.

efficient stepsize control

The explicit form retains simplicity, and embedded formulas permit an efficient stepsize control. Efficiency can be further improved when the user provides an upper bound on the timestep stability restriction for the forward Euler method.

Adaptive splitting timestepping strategy

We adjust the size of splitting steps using the following roughness $w(t)$-dependent monitor function

$$\Delta t = \max\left(\Delta t_{\min}, \frac{\Delta t_{\max}}{\sqrt{1+\alpha|w'(t)|^2}}\right), \quad \alpha = \text{constant}, \quad w(t) = \sqrt{\frac{1}{|\Omega|}\int_\Omega [u(\boldsymbol{x},t)-\bar{u}(t)]^2\,d\boldsymbol{x}}, \quad \text{where } \bar{u}(t) = \frac{1}{|\Omega|}\int_\Omega u(\boldsymbol{x},t)\,d\boldsymbol{x}$$

Numerical examples

1. MBE equation ($\delta = 0.1$) subject to the initial condition

$$u(\boldsymbol{x},0) = 0.1(\sin 3x\sin 2y + \sin 5x\sin 5y), \quad \boldsymbol{x}\in[0,2\pi]^2$$

- constant splitting timestep $\Delta t = 10^{-3}$

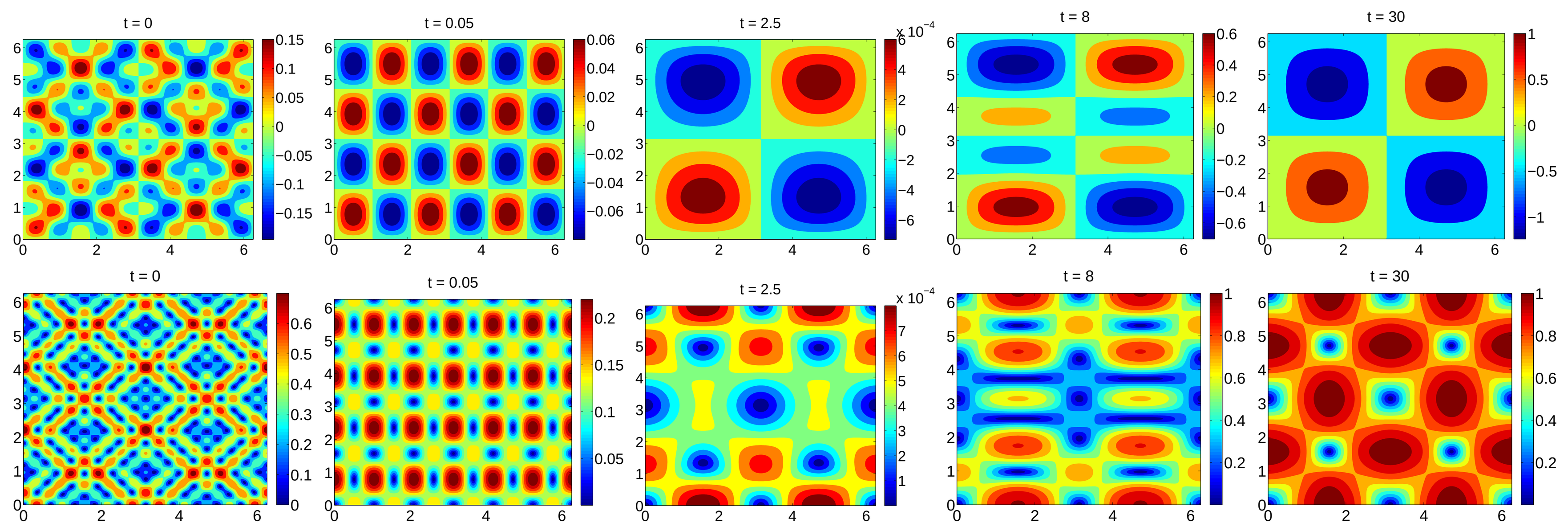

Figure 4: MBE: (first row) Contour plots of u; (second row) Contour plots of $|\nabla u|$

- adaptive splitting timestepping leads to similar results as above ones.

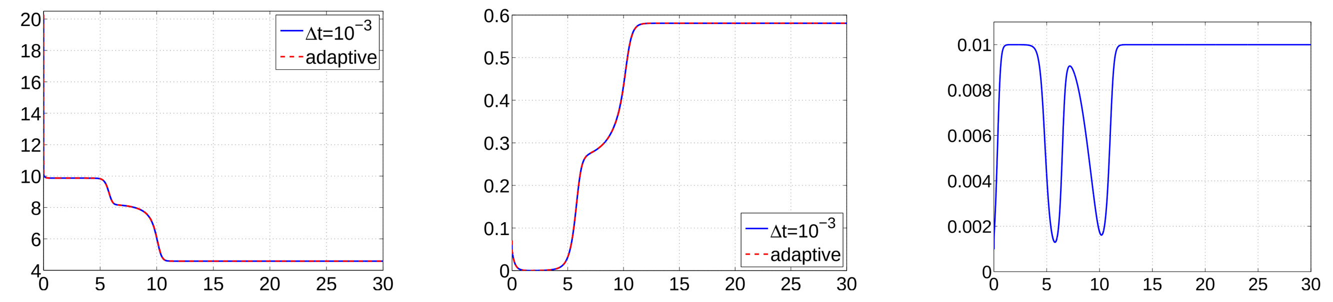

Figure 5: MBE: (left) Energy evolution; (middle) Roughness development; (right) Splitting step evolution. $\Delta t = 10^{-3}$ (solid line) and adaptive splitting timestepping with $\Delta t_{\min} = 10^{-3}$, $\Delta t_{\max} = 10^{-2}$ and $\alpha = 10^3$ (dashed line).

2. MBE equation ($\delta = 1$) subject to the initial condition uniformly distributed random number in the range $[-0.001, 0.001]$ to each grid point value of $u(\boldsymbol{x},0)$, $\boldsymbol{x}\in[0,1000]^2$

- constant splitting timestep $\Delta t = 10^{-1}$

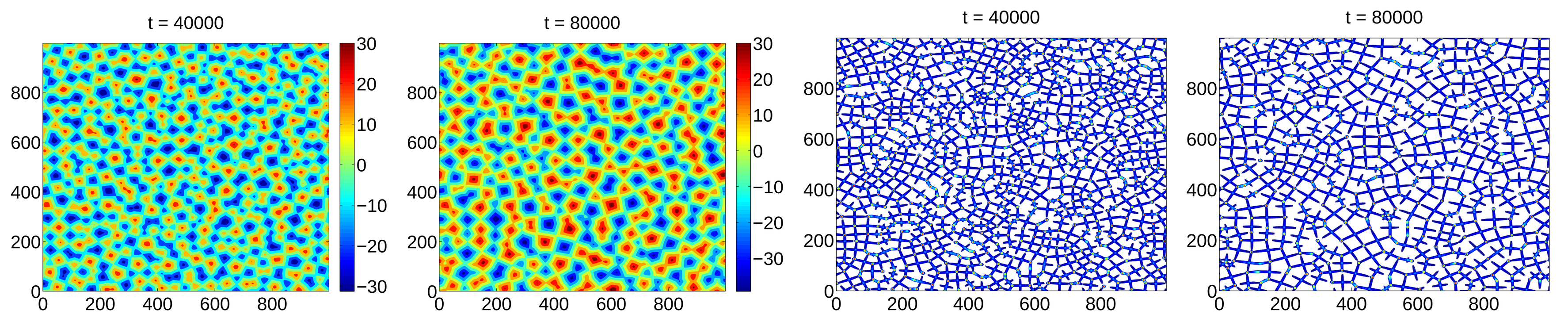

Figure 6: MBE: (left two) Contour plots of solution profile; (right two) Contour plots of free energy.

3. CH equation ($\delta = 0.01$) subject to the initial condition

$$u(x,y,0) = 0.05\sin x\sin y + 0.001, \quad \boldsymbol{x}\in[0,2\pi]^2$$

- constant splitting timestep $\Delta t = 10^{-3}$

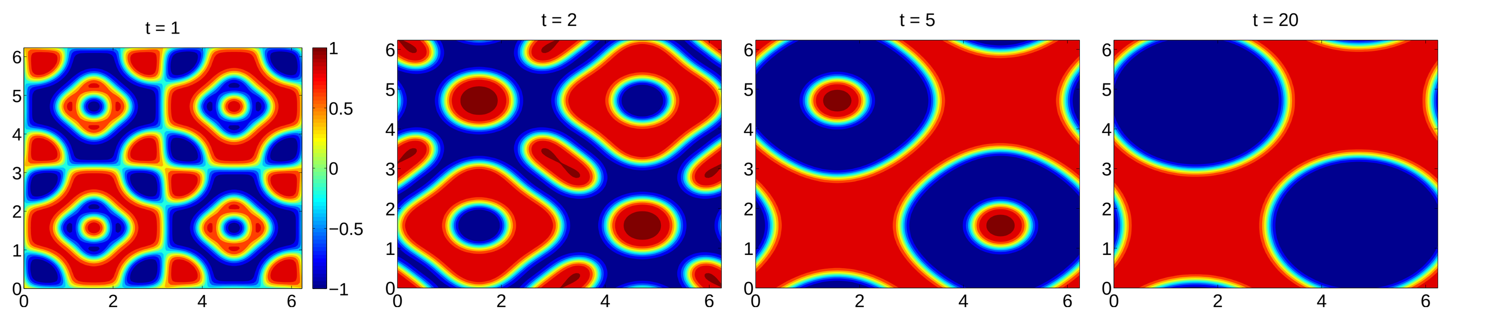

Figure 7: CH: Contour plots of u computed with $\Delta t = 10^{-3}$.

- adaptive splitting timestepping leads to similar results as above ones.

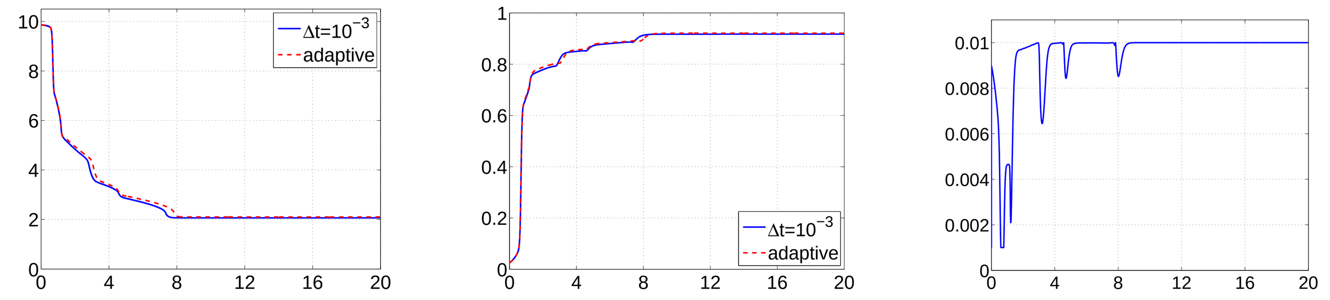

Figure 8: CH: (left) Energy evolution; (middle) Roughness development; (right) Splitting step evolution. $\Delta t = 10^{-3}$ (solid line) and adaptive splitting timestepping with $\Delta t_{\min} = 10^{-3}$, $\Delta t_{\max} = 10^{-2}$ and $\alpha = 10^2$ (dashed line).

References

[1] J. W. Cahn and J. E. Hilliard, *Free energy of a nonuniform system. I. interfacial free energy*, J. Chem. Phys., 28 (1958), pp. 258–267.

[2] A. Chertock and A. Kurganov, *On Splitting-Based Numerical Methods for Convection-Diffusion Equations*, Quaderni di Matematica, 24 (2009), pp. 303–343.

[3] X. Feng, T. Tang, and J. Yang, *Long time numerical simulations for phase-field problems using p-adaptive spectral deferred correction methods*, SIAM J. Sci. Comput., 37 (2015), pp. A271–A294.

[4] A. Medovikov, *High order explicit methods for parabolic equations*, BIT, 38 (1998), pp. 372–390.

[5] T. Cool et al, *Gibbs: Phase equilibria and symbolic computation of thermodynamic properties*, Calphad, 34 (2010), pp. 393–404

Acknowledgements

The work of Y. Cheng, A. Kurganov and Z. Qu was supported in part by the NSF Grant # DMS-1115718.

This poster is produced for the *SCALA 2015 : SCIENTIFIC COMPUTING AROUND LOUISIANA*, March 20-21, 2015.

Author: Zhuolin Qu, *Author contact*: ✉ zqu1@tulane.edu.

Copyright information:
All the figures on numerical simulations are created by MATLAB by the author of the poster.
The logo of Tulane University is downloaded from `http://tulane.edu/tulane/news/style/logos/downloads.cfm` and is available for use on Tulane University print publications.
The poster is typeset using LaTeX `beamerposter` package.